Astron. Astrophys. 305, 245–254 (1996)

ASTRONOMY
AND
ASTROPHYSICS

Empirical study of departures from the excitation equilibrium of Fe I in metal-poor stars*

P. Magain[1]** **and G. Zhao**[2]

[1] Institut d'Astrophysique, Université de Liège, 5, avenue de Cointe, B-4000 Liège, Belgium
[2] Beijing Astronomical Observatory, Chinese Academy of Sciences, Beijing 100080, People's Republic of China

Received 6 September 1994 / Accepted 19 April 1995

Abstract. A detailed analysis of neutral iron lines in a sample of 13 metal-poor dwarfs and subgiants is carried out on the basis of high resolution spectra obtained with the ESO Coudé Echelle Spectrometer. The deduced iron abundance is found to depend on the excitation potential of the line used, higher excitation lines generally indicating higher abundances. This could be caused by departures from the local thermodynamic equilibrium (LTE) or by temperature inhomogeneities in the stellar atmospheres. The dependency of this effect on the stellar atmospheric parameters is investigated. From the comparison of iron lines with lines of other elements, it is concluded that the low excitation Fe I lines are much more affected than the high excitation lines. The consequences of these effects for the classical abundance analyses are examined. It is found that they may explain, at least in part, some previously reported discrepancies between the results of different authors[1].

Key words: stars: abundances; population II – Galaxy: abundances

1. Introduction

Until recent years, the accuracy of most abundance analyses of metal-poor stars was generally limited by the low S/N of the spectra and by the poor quality of the oscillator strengths available. This situation has now completely changed, due mainly to two factors. First, high accuracy oscillator strengths have become available for a significant number of lines, mostly under the impulse of Blackwell and his collaborators at Oxford. Secondly, the combination of large telescopes with high resolution spectrographs and solid-state detectors has allowed to improve drastically the quality of the stellar spectra, especially for rather faint stars.

Given these improvements on the experimental and observational sides, the accuracy of the derived abundances is now limited by the uncertainties in the methods of analysis (see Gustafsson 1988, for a discussion of these problems). Among these uncertainties, one may mention the difficulty to get accurate atmospheric parameters (especially the effective temperature, which plays the most critical role) and the consequences of adopting the classical assumptions of local thermodynamic equilibrium (LTE) and plane parallel model atmosphere (PPMA), the latter meaning that temperature inhomogeneities are neglected.

The metal-poor stars, besides their crucial importance for the study of the early stages of galactic evolution, constitute excellent laboratories for testing these two approximations. Indeed, the lower opacity of their atmospheres means:
(1) higher UV fluxes, thus making departures from LTE more likely;
(2) a deeper photosphere reaching the convection zone, therefore increasing the importance of temperature inhomogeneities.

The validity of the classical assumptions may be investigated along two main lines. (1) One can adopt the direct – theoretical – approach, by building sophisticated hydrodynamical model atmospheres (as was initiated by Nordlund 1984) and making use of full statistical equilibrium calculations with extensive model atoms (see, e.g., Gigas 1988). Apart from requiring very heavy and costly computations, these studies still suffer from important uncertainties (let us just mention unknown cross sections for the statistical equilibrium calculations or some drastic, but necessary, simplifications in the hydrodynamical equations). (2) Given these limitations, it appears useful also to follow an alternative – empirical – approach. One can adopt the classical assumptions of LTE and PPMA, derive abundances from different lines of the same element and then check for consistency: all lines of the same element should lead to the same abundance. If not, this means that at least one of the assumptions is not valid. Such an approach is purely empirical in the sense that neither departures from LTE nor any inhomogeneous model are included

Send offprint requests to: P. Magain

* Based on observations carried out at the European Southern Observatory, La Silla, Chile

** Chercheur Qualifié au Fonds National Belge de la Recherche Scientifique

[1] Table 4 is available electronically at the CDS via anonymous ftp 130.79.128.5

Table 1. Photometric data

HD	V	$V-K$	$b-y$	m_1	c_1
3567	9.25	1.34	0.334	0.087	0.334
25704	8.12	1.53	0.371	0.119	0.273
122196	8.74	1.43	0.349	0.051	0.331
126793	8.19	1.44	0.370	0.127	0.290
132475	8.56	1.61	0.390	0.075	0.282
152924	8.02	1.24	0.318	0.118	0.376
160617	8.74	1.39	0.343	0.059	0.334
166913	8.23	1.31	0.326	0.079	0.303
189558	7.74	1.55	0.385	0.119	0.269
193901	8.67	1.50	0.376	0.108	0.210
194598	8.35	1.37	0.342	0.091	0.270
196892	8.24	1.37	0.349	0.099	0.303
199289	8.29	1.42	0.368	0.093	0.264

in the computations. It obviously requires very high quality data as each line has to be used by itself: the abundance cannot be averaged over many lines in order to reduce the uncertainties.

Very few past investigations have addressed this problem of consistency of the line abundances. We may mention the analysis of Pollux by Ruland et al. (1980) who found such inconsistencies for Ti, Cr and Fe and a similar work for Procyon by Steffen (1985). Some trends with excitation potential were also reported by Peterson (1988) in metal-poor giants.

In a preliminary analysis of one metal-poor subgiant by Magain (1988), the abundances of several elements (most notably Fe I, but also O I and Ca I) were found to depend on the excitation potential of the lines used to derive them. The aim of the present paper is to extend this empirical analysis to a sample of thirteen metal-poor dwarfs and subgiants, in an attempt to better assess the importance of this effect as a function of the stellar atmospheric parameters and, hopefully, to help improve our understanding of the physics of metal-poor stellar atmospheres.

2. Observations and reductions

The observations were carried out with the Coudé Echelle Spectrometer (CES) fed by the 1.4 m Coudé Auxiliary Telescope (CAT) at the European Southern Observatory (La Silla, Chile). The short camera was used with a high resolution (15×15 μm pixels) RCA CCD. The entrance slit width was set to 2 arc seconds, in order to match the pixel size, thus giving a resolving power of the order of 55000. The exposure times were chosen to reach a signal-to-noise ratio around 200 in all spectral regions.

Thirteen stars were selected to cover a reasonable range in metallicity ($-2 \lesssim$ [Fe/H] $\lesssim -1$), effective temperature (5500 K $\lesssim T_{\rm eff} \lesssim$ 6100 K) and surface gravity ($3.5 \lesssim \log g \lesssim 4.6$). The list of program stars, along with some basic photometric data, is given in Table 1.

The spectra were collected during three observing runs, in August 1987 (10 nights), July 1988 (6 nights) and August 1989 (7 nights), the last two having been carried out in remote control from the ESO headquarters in Garching bei München, FRG. All stars were observed in four wavelength bands, each band having a width of 40 to 50 Å. These spectra were centered around 5197, 5254, 5860 and 6485 Å. Additional spectra were also obtained around 6589 Å for seven stars and in the 6150 Å region (in the context of another program) for eleven stars.

The data reduction was carried out with the help of the IHAP facility running on a HP 1000 computer at ESO, Garching. It consisted in:

(1) background subtraction, on the basis of the mean level measured on the parts of the CCD not illuminated by the stellar light, thus including electronic bias and dark current as well as any source of diffuse light;

(2) flat-fielding, using the spectrum of an internal lamp for the two shorter wavelengths, and the light of either an external lamp (as reflected by a white screen in the dome) or a blue star in the case of the redder wavelengths, the latter method allowing a better correction of the interference fringes;

(3) wavelength calibration, using the stellar lines themselves to define the calibration curve, thus automatically correcting for the radial velocity;

(4) definition of the continuum, in the form of a low order Spline fitted through a number ($\sim$ 20) of pre-defined continuum windows;

(5) equivalent width measurement, by gaussian fitting and by direct integration, the first method being preferred for the weak lines and the second in the case of the stronger ones (for which the non-gaussian damping wings contribute significantly to the equivalent width).

All lines were then checked for possible contamination by telluric lines (mainly water vapor in the redder spectral regions) and were rejected in case of blending. Moreover, in order to get the highest accuracy in the deduced abundances, only the lines with EWs less than 70 mÅ were considered. The measured equivalent widths (EWs) for all lines used in the present analysis are listed in Table 4. The internal accuracy of these EWs was estimated by comparing the measurements on two independent spectra of the 5197 Å region in HD 166913, which led to a one sigma uncertainty of about 1.5 mÅ for lines of intermediate strength (20 to 60 mÅ). This is to be compared with an 'ideal' uncertainty of the order of 0.5 mÅ if photon noise alone contributed to the EW errors. Additional sources of error may include readout noise of the CCD, undetected hits by cosmic ray particles, weak blends or uncertainties in the location of the continuum.

3. Determination of the atmospheric parameters

The line analysis is based on model atmospheres computed with a version of the MARCS program (Gustafsson et al. 1975) including some additional opacity in the UV spectral region (Magain 1983).

As already mentioned, any accurate abundance analysis requires a precise knowledge of the stellar atmospheric parameters. Moreover, our aim being to investigate the possibility that iron lines are affected by departures from the classical assumptions, these lines should not be used to determine any of the

Table 2. Atmospheric parameters

HD	$T_{\rm eff}$	$\log g$	[Fe/H]	$v_{\rm turb}$	δ[Fe/H]
3567	5990	3.9	−1.4	1.15	+0.03±0.01
25704	5710	3.9	−1.1	1.35	+0.18±0.04
122196	5860	3.6	−2.1	1.50	+0.21±0.05
126793	5780	3.9	−1.1	1.30	+0.07±0.04
132475	5580	3.5	−1.7	1.00	+0.14±0.03
152924	6120	3.9	−1.2	1.25	+0.28±0.04
160617	5920	3.7	−2.0	1.60	+0.17±0.06
166913	6030	4.0	−1.8	1.40	+0.25±0.07
189558	5650	3.9	−1.0	1.25	+0.11±0.02
193901	5720	4.6	−1.2	0.35	−0.11±0.04
194598	5930	4.1	−1.4	1.00	+0.17±0.02
196892	5940	4.0	−1.2	1.15	+0.18±0.06
199289	5840	4.2	−1.1	0.80	+0.08±0.01

model parameters. Indeed, their use could be expected to lead to some compensation or masking of departures from the classical assumptions by appropriate changes in the model parameters.

3.1. Effective temperature

The effective temperature $T_{\rm eff}$ was determined from the Strömgren b–y and Johnson V–K colours, using the calibrations of Magain (1987). The sources of b–y measurements are Carney (1983), Lindgren (private communication), Olsen (private communication) and Schuster & Nissen (1988). The V–K colours were taken from Carney (1983) or obtained by us with the ESO 1m telescope on La Silla. The adopted effective temperature is a mean of the two determinations and is listed in Table 2. The agreement between the two colour temperatures is excellent, the mean difference $T_{\rm eff}(b-y) - T_{\rm eff}(V-K)$ amounting to 9 K, with a scatter of 39 K in the individual determinations.

3.2. Surface gravity

Obviously, the usual method of gravity determination from the iron ionization equilibrium is not appropriate in the present context. However, as we are primarily interested in Fe I lines, which are rather insensitive to surface gravity, the choice of this parameter is not very critical. The surface gravity $\log g$ was thus estimated from the Strömgren c_1 index, using the calibration of VandenBerg & Bell (1985) for the adopted effective temperature and metallicity.

3.3. Metallicity

Again, this is not a critical parameter in metal-poor stars model atmospheres as the continuous opacity is dominated by the contribution of the negative hydrogen ion. The model metallicity was thus taken from previously published analyses, if available. Otherwise, it was estimated from the Strömgren m_1 index.

3.4. Microturbulent velocity

To obtain a microturbulent velocity as independent as possible from any non-LTE effect, we decided to use a group of lines of the same element, with the same lower excitation potential (EP). As any accurate determination also requires a set of lines with precise oscillator strengths covering a significant range in EW, only the Ca I lines with 2.52 eV EP were found to satisfy all the requirements. They were supplemented by the strong Ca I line at 6162 Å (EP = 1.90 eV) in the three stars with the weakest lines for which the 2.52 eV lines are too weak to be reliable microturbulent velocity indicators.

The Ca I oscillator strengths were taken from Smith & Raggett (1981). The damping constants γ_6 were computed from the Unsöld formula (Gray 1976) multiplied by an enhancement factor f_6 determined by forcing the calculated solar EWs to agree with the observed ones (the latter being taken from Smith 1981). The Holweger-Müller (1974, HM) model was used for the sun and the solar calcium abundance was adopted from Smith (1981).

The f_6 values for different lines of a given multiplet were then averaged, with a weight equal to the inverse square of the error in f_6 caused by the uncertainty in the solar EW. Our results are f_6 = 0.8 for multiplet 18, 1.4 for multiplet 20 and 2.0 for multiplet 22, in good agreement with the values of Smith (1981).

The microturbulent velocity $v_{\rm turb}$ was then chosen to remove any dependency of the computed line abundance on the EW, using the procedure suggested by Magain (1984b) in order to avoid systematic errors.

The results are gathered in Table 2. For two stars (HD 152924 and HD 189558) for which we have no spectrum in the 6150 Å region, a value of 1.25 km/s has been adopted and is compatible with the few Ca I lines available.

4. Oscillator strengths and damping constants

The oscillator strengths of the Fe I lines were, whenever possible, taken from the very accurate work of Blackwell et al. (1979a, b, 1980, 1982). For these lines, the damping enhancement factor f_6 was determined following Simmons & Blackwell (1982), i.e. by comparing the wings of strong lines in the solar spectrum with weaker lines from the same multiplet.

Unfortunately, the Blackwell et al. oscillator strengths have been measured for rather low excitation lines only (EP < 2.6 eV). No work of comparable accuracy has been carried out for high excitation lines. Thus, we decided to rely on the solar spectrum for the determination of these oscillator strengths, therefore introducing an additional source of uncertainty. Indeed, as we are interested in metal-poor stars, the lines of suitable strength in the stellar spectra are rather strong in the solar spectrum and, thus, quite sensitive to damping. The damping constant being largely unknown, it has to be determined.

This was done in the following way. We considered a set of lines originating from the same lower level but having different strengths. We assumed that a single damping enhancement factor can be applied to them and that any departure from LTE would affect all these lines in the same way. (This is confirmed *a posteriori* by our results which show the departures from excitation equilibrium to depend smoothly on the line EP). The lines being weak in the metal-poor stars, their EWs are fairly independent of the damping constants and, thus, the stellar spectra can be used to determine the relative oscillator strengths. The latter being known, the damping enhancement factor can then be determined by forcing the lines of different strengths in the sun to give the same solar abundance.

Only one such set of lines is available in our spectra. It consists of the three lines at 5852.2, 5859.6 and 5862.4 Å originating from a level at 4.55 eV. The solar equivalent widths, measured on the Liège atlas (Delbouille et al. 1973), amount respectively to 42.4, 79.2 and 94.5 mÅ. Nine stars could be used to determine the relative gf values, which are slightly dependent on the adopted damping constant. An iterative procedure had thus to be used, where an initial value of f_6 was adopted and then the relative $\log gf$ determined from which a better f_6 was deduced, and so on until convergence. The resulting f_6 turned out to be 1.4, with an uncertainty of the order of 0.2 – 0.3, dominated by the uncertainty on the solar EWs (and not on the relative gf values).

On the basis of this result, and on the hypothesis of a rather smooth variation of f_6 with EP (see Simmons & Blackwell 1982), this value of 1.4 was adopted for all lines with EP higher than 2.6 eV. The solar spectrum was then used to determine the line oscillator strengths. The solar iron abundance was computed from weak lines with accurate gf values, which gave $\log(A_{Fe})$ = 7.68 in the usual scale where the logarithm of the hydrogen abundance is set to 12.00. The solar HM model was used in all these computations, with a constant microturbulent velocity of 0.85 km/s at the center of the disk. The adopted line data are listed in Table 3.

Table 3. Line data

Elem.	λ	χ_{exc}	$\log gf$	f_6	$W_\lambda(\odot)$
Fe I	5194.95	1.56	−2.090	1.2	–
Fe I	5196.07	4.26	−0.850	1.4	79.0
Fe I	5198.72	2.22	−2.135	1.2	–
Fe I	5216.28	1.61	−2.150	1.2	–
Fe I	5217.40	3.21	−1.060	1.4	124.0
Fe I	5242.50	3.63	−1.190	1.4	89.3
Fe I	5243.78	4.26	−1.100	1.4	64.1
Fe I	5247.06	0.09	−4.946	1.0	–
Fe I	5250.22	0.12	−4.938	1.0	–
Fe I	5852.22	4.55	−1.280	1.4	42.4
Fe I	5856.09	4.29	−1.670	1.4	34.3
Fe I	5859.59	4.55	−0.660	1.4	79.2
Fe I	5862.36	4.55	−0.450	1.4	94.5
Fe I	6469.19	4.83	−0.760	1.4	59.9
Fe I	6475.63	2.56	−2.930	1.4	54.8
Fe I	6481.88	2.28	−2.984	1.2	–
Fe I	6494.99	2.40	−1.273	1.3	–
Fe I	6496.47	4.79	−0.710	1.4	65.5
Fe I	6498.95	0.96	−4.699	1.1	–
Fe I	6569.22	4.73	−0.570	1.4	78.0
Fe I	6575.04	2.59	−2.770	1.4	61.8
Fe I	6592.93	2.73	−1.650	1.4	120.4
Fe I	6593.88	2.43	−2.422	1.3	–
Fe I	6597.57	4.79	−1.060	1.4	44.7
Fe I	6609.12	2.56	−2.730	1.4	65.5
Ca I	5261.71	2.52	−0.579	1.4	–
Ca I	6161.29	2.52	−1.266	2.0	–
Ca I	6162.18	1.90	−0.090	2.3	–
Ca I	6166.44	2.52	−1.142	2.0	–
Ca I	6169.04	2.52	−0.797	2.0	–
Ca I	6169.56	2.52	−0.478	2.0	–
Ca I	6471.67	2.52	−0.686	0.8	–
Ca I	6493.79	2.52	−0.109	0.8	–
Ca I	6499.65	2.52	−0.818	0.8	–
Ti I	5192.98	0.02	−1.006	1.5	–
Ti I	5210.39	0.05	−0.884	1.5	–
Cr I	5247.57	0.96	−1.627	1.5	–

5. Results

5.1. Departures from the excitation equilibrium and their variation with the atmospheric parameters

The iron abundance was deduced from each line (see Table 4, available electronically) under the assumption of LTE and the results were checked for consistency. It was generally found that the line abundance varies as a function of EP, confirming the results of Magain (1988). A few representative cases are displayed in Figs. 1 to 3: HD 25704 which is rather typical of the sample studied here, with an abundance increasing moderately as a function of the line EP; HD 152924 which shows the strongest slope, and HD 193901, the only star for which the line abundance was found to decrease with increasing EP.

The variation of the deduced Fe I abundance with the lower EP of the line considered is thus a rather general phenomenon in metal-poor dwarfs. To better quantify this effect, we need to define a criterion which should be as sensitive as possible to the variation of the line abundance as a function of EP and as insensitive as possible to all other parameters and approximations. The adopted criterion is the difference in abundance as indicated by (1) the 3 lines with 4.5 eV EP and (2) the 2 lines with 0.1 eV EP. These two sets were chosen for the following reasons:
- large difference in EP;
- well determined oscillator strengths and damping constants;
- similar equivalent widths (and thus insensitivity to the adopted microturbulent velocity);
- suitable strength in most of the stars.

These abundance differences δ[Fe/H] are listed in Table 2. The one sigma error bars have been determined on the basis of the dispersion in the abundances indicated by the different lines with the same EP. They correspond to the standard deviation of the mean values. For HD 160617, no 4.5 eV line could be

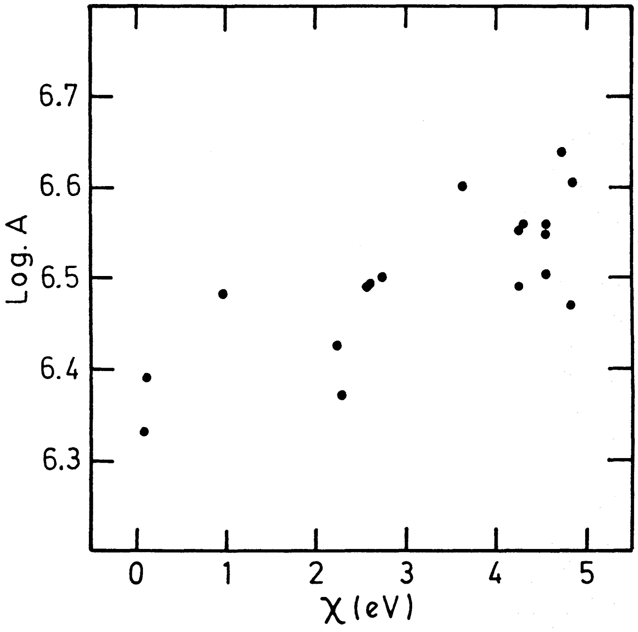

Fig. 1. Plot of Fe abundance versus excitation potential for HD 25704

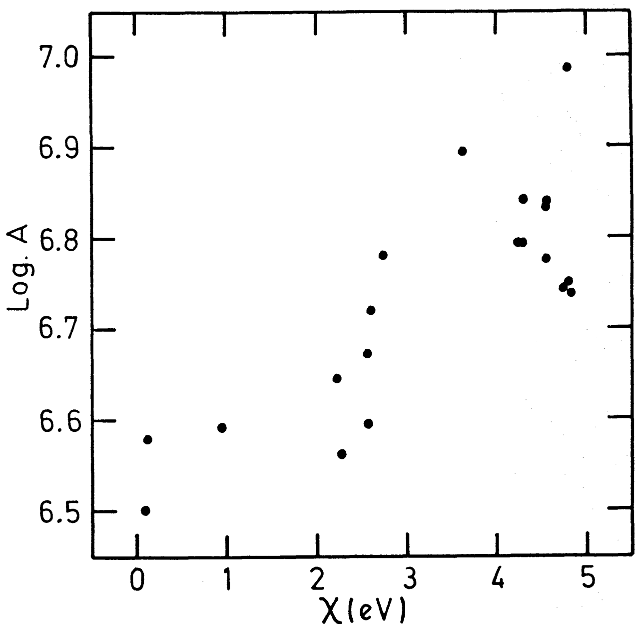

Fig. 2. Plot of Fe abundance versus excitation potential for HD 152924

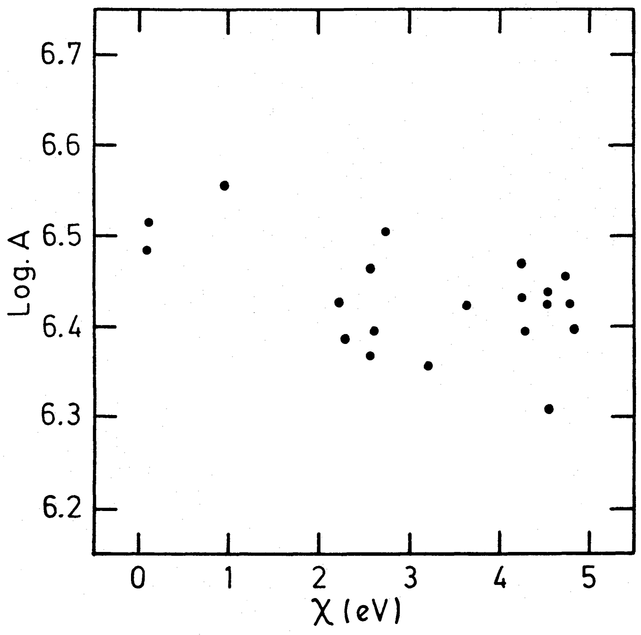

Fig. 3. Plot of Fe abundance versus excitation potential for HD 193901

used: they are either too weak or blended with telluric water vapor lines. The abundance was thus deduced from lines of neighbouring EP (4.26 and 4.29 eV) after checking that, in all other stars, these lines give abundances in agreement with the 4.5 eV lines.

Figure 4 shows these abundance differences plotted in the ($T_{\rm eff}$, $\log g$) diagram, which is related to the Hertzprung-Russell diagram. Very tentative curves of equal δ[Fe/H] have been drawn. They give a satisfactory representation of the variation of δ[Fe/H] with $T_{\rm eff}$ and $\log g$ for all but two stars (namely HD 3567 and HD 25704; note, however, that HD 3567 is suspected to be a binary, Carney 1983). It should be stressed that the size of the dots in Fig. 4 does not correspond to the uncertainty in the atmospheric parameters, especially in the case of the surface gravity for which the error bar may be of the order of 0.2 – 0.3 dex. On the basis of the present data, we would tentatively suggest that δ[Fe/H] increases with decreasing surface gravity and with increasing effective temperature, in the range of parameters considered here. This behavior is reminiscent of departures from LTE, which are expected to increase as the gas pressure lowers and as the UV flux becomes stronger.

It may be intriguing to note that Fig. 4 indicates a δ[Fe/H] of 0.0 for the metal-poor stars having the solar effective temperature and surface gravity. It therefore suggests that the departures from excitation equilibrium depend on temperature and gravity, but not on metal abundance.

5.2. Which lines are the correct abundance indicators ?

Having shown that the use of Fe I lines with various excitation potentials leads to different iron abundances, the next step would consist in determining which lines, if any, indicate the correct abundance. For this purpose, we determined the calcium abundance relative to iron in two cases: (1) when the iron abundance is deduced from low excitation lines and (2) when it is given by high excitation lines. The results are plotted in Fig. 5 as a function of δ[Fe/H] as defined in the preceding section. It is seen that [Ca/Fe] is strongly correlated with δ[Fe/H] in the first case, i.e. when then 0.1 eV Fe I lines are used, while no correlation is present when the 4.5 eV lines are considered. This means that, when the low EP Fe I lines indicate a lower iron abundance than the high EP lines, they also indicate a lower than average [Fe/Ca]. On the contrary, the high EP Fe I lines always indicate

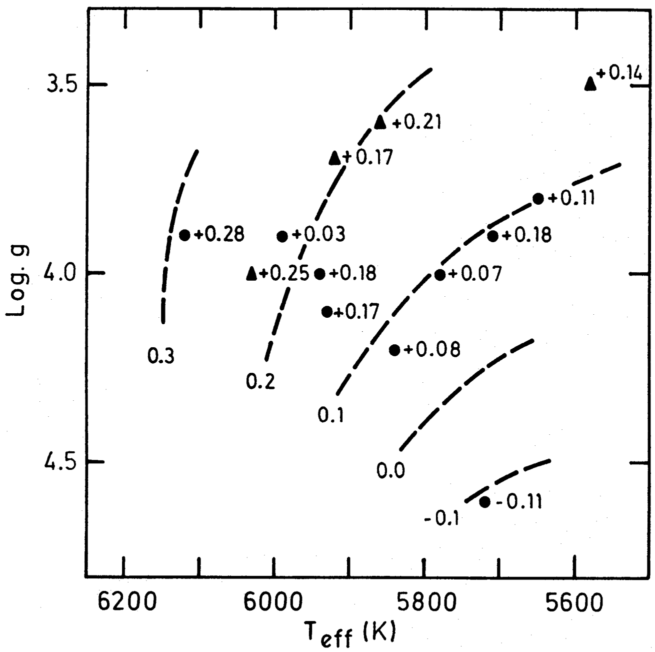

Fig. 4. The abundance discrepancies δ[Fe/H] are plotted in the ($T_{\rm eff}$, $\log g$) diagram. Circles correspond to stars with [Fe/H] > -1.5 while triangles indicate stars with [Fe/H] < -1.5. Tentative loci of constant δ[Fe/H] are also shown

the same [Fe/Ca], irrespective of the slope in the (EP, $\log A$) diagram. One can thus conclude that, either the Ca I lines suffer from exactly the same departures from excitation equilibrium as the 4.5 eV Fe I lines, or the latter are the correct abundance indicators.

While the first possibility appears at first sight very unlikely, it cannot be immediately ruled out. Indeed, both calcium and iron are mostly ionized in the stellar atmospheres considered. In such a case, the temperature sensitivity of weak neutral lines is a function of $I - \chi$, where I is the first ionization potential and χ the line EP. Thus, the 2.5 eV Ca I lines have the same temperature sensitivity as Fe I lines of 4.3 ($\simeq$ 4.5) eV EP. So, the lack of correlation between [Ca/Fe] and δ[Fe/H] when high EP Fe I lines are used would be naturally explained if the departures from excitation equilibrium were due to temperature errors (e.g. a wrong choice of the star's effective temperature, a wrong $T(\tau)$ relation in the models or the effect of temperature inhomogeneities). The last two possibilities are just the kind of effects we are looking for. On the other hand, as far as effective temperature errors are concerned, changes of more than 400 K would be necessary in some cases to remove the slopes. Such changes are far above the expected uncertainty in the photometric $T_{\rm eff}$ determination. Although we consider that possibility as highly unlikely, it will be discussed more extensively in the next section.

If the comparison of the Fe I lines with the 2.5 eV Ca I lines allows to identify the low EP lines as affected by departures from the excitation equilibrium, this comparison does not provide any clear indication as to the cause of these departures. Further insight may be gained by comparing the Fe I lines with lines of other elements having different temperature sensitivities. Three such lines are available on our spectra: two Ti I lines with $\chi \simeq 0$ eV, thus having a temperature sensitivity similar to 1 eV Fe I lines and one Cr I line with $\chi \simeq 1$ eV, which has a temperature sensitivity corresponding to 2 eV Fe I lines. Although the correlations are not as well defined as in the case of calcium, both the Ti I and Cr I lines indicate abundances compatible with the high excitation Fe I lines, *not* with the Fe I lines having the same temperature sensitivity (Fig. 6). This is a strong indication that departures from LTE, rather than temperature errors, contribute significantly to the observed effect.

Let us mention that the fact that the correlations are slightly less well defined when Ti I and Cr I lines are used as when Ca I lines are considered may be explained in part by the smaller number of lines but may also indicate that some non-LTE effects are present in the low excitation Ti I and Cr I lines too.

6. Assumptions and uncertainties

The derived abundance discrepancies δ[Fe/H] are affected by a number of uncertainties, which may be considered as belonging to three main classes, according to their consequences on the above conclusions. These three classes of errors are discussed in turn.

6.1. Errors affecting a single line in a single star

This class is mainly represented by the random errors in the measured EWs. These errors contribute to the dispersion in our resulting δ[Fe/H], but should not introduce any systematic effect. They can be estimated from the scatter in the individual line abundances at a given EP. The corresponding uncertainties in δ[Fe/H] are listed in Table 2. They range from 0.01 to 0.07 dex, with a typical value of 0.04 dex.

6.2. Errors affecting all lines in a single star

A wrong choice of the atmospheric parameters for one star would cause errors in the abundances derived from all lines. These errors generally varying from line to line, a wrong value of δ[Fe/H] might result.

The effect of errors in the adopted atmospheric parameters was investigated by repeating the analysis of HD 194598 (a typical star in our sample) with different choices of $T_{\rm eff}$, $\log g$, [Fe/H] and $v_{\rm turb}$. As might be expected, only the effective temperature plays a critical role. Significant changes of the other three parameters (0.5 dex in $\log g$ and [Fe/H], 0.5 km/s in $v_{\rm turb}$) leave δ[Fe/H] unchanged within 0.01 dex. On the other hand, a variation of 100 K in $T_{\rm eff}$ translates into a change of 0.07 dex in δ[Fe/H].

One might thus argue that the abundance discrepancies are due to errors in the adopted effective temperatures. The mean value of δ[Fe/H] for our sample of 13 stars amounts to 0.14 dex. If due to a systematic error in the $T_{\rm eff}$ calibration, such an error would have to be of the order of 200 K. This is much

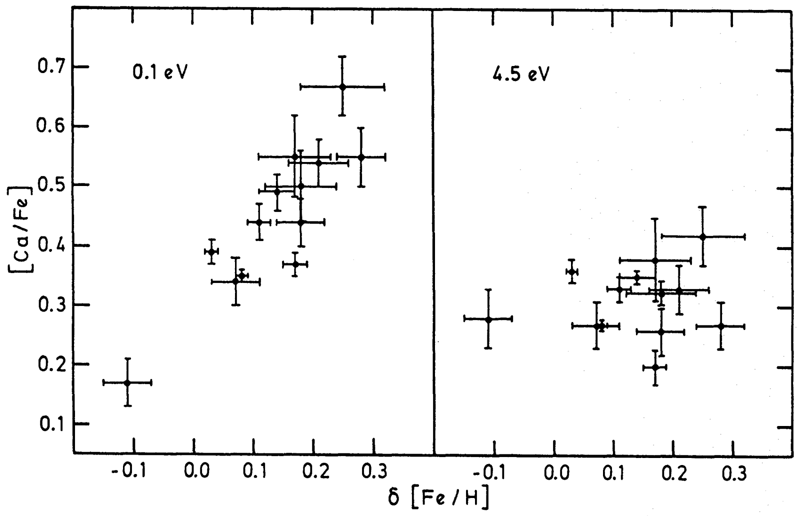

Fig. 5. Plot of [Ca/Fe] versus abundance discrepancy δ[Fe/H] using either the 0.1 eV Fe I lines (left part) or the 4.5 eV Fe I lines (right part). The error bars correspond to the standard deviation of the mean values

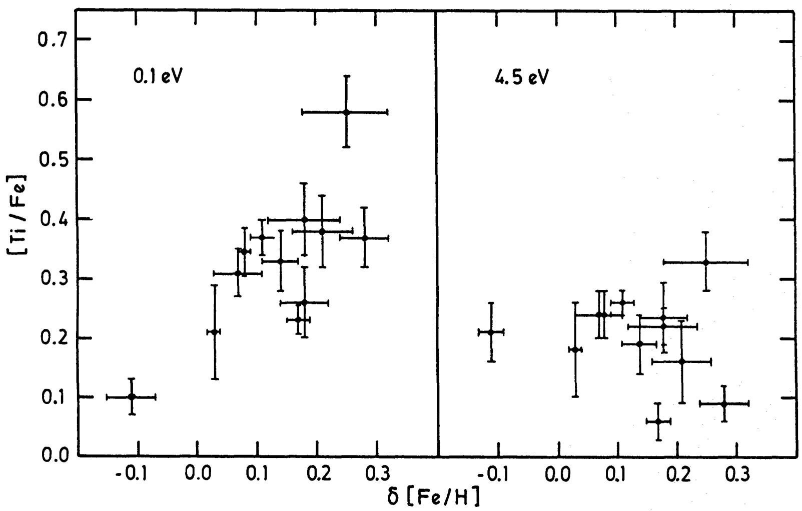

Fig. 6. Plot of [Ti/Fe] versus abundance discrepancy δ[Fe/H] using either the 0.1 eV Fe I lines (left part) or the 4.5 eV Fe I lines (right part). The error bars correspond to the standard deviation of the mean values

larger than the discrepancy between different calibrations of the colour indices: as an example, the calibrations of Carney (1983) and Magain (1987) agree within 30 K in the temperature and metallicity ranges covered by our program stars.

However, some doubts on the validity of the calibration of Magain (1987, M87) were recently raised by King (1993), who argued that this calibration might be wrong by 150 K. King's discussion is essentially based on an erroneous use of the calibration: he bases his arguments on the formula (2) of M87, which is a mean curve for halo stars ([Fe/H] < -1) and uses it at [Fe/H] = -0.5. Formula (15) has to be preferred, as it contains an explicit metallicity dependence, but should nevertheless not be used outside its range of validity, i.e. for halo dwarfs. This is that formula which is used in the present paper, as well as in our previous works. Comparison of the empirical calibration (15) of M87 with the recent theoretical calibration of Edvardsson et al. (1993) for [Fe/H] = -1, that is, for the only metallicity where these calibrations are both valid, shows a quasi constant difference of 60 K, which is thus an estimate of the maximum systematic error in any of these calibrations.

More doubts on the determination of effective temperatures from colour indices were raised by Fuhrmann et al. (1994, FAG). These authors, who determined the effective temperatures of a large number of cool dwarf stars from fits of the Balmer lines, argue that, due to reddening and to problems in the colour transformations, the photometric temperatures can only be used in a statistical sense and cannot provide accurate effective temperatures for individual stars.

Out of our 13 stars, 8 are in the sample of FAG. By comparing their temperatures estimates $T(FAG)$ with our own determinations $T(MZ)$, we find a systematic difference of

$$T(MZ) - T(FAG) = 110\ (\pm 100)\ \mathrm{K}$$

Thus, the temperatures deduced from the Balmer lines are lower on the average (indeed, for all but one star) than the photometric values. If our program stars were affected by reddening, one would expect the photometric temperatures to be *underestimated*, while the comparison shows that they are *higher* than the FAG values. Therefore, reddening cannot explain the observed discrepancy.

Moreover, the scatter of 100 K in the temperature differences is entirely compatible with the uncertainties listed in FAG (ranging from 84 to 200 K, with a mean value of 115 K). It indicates that most of the scatter can be attributed to the FAG temperatures and confirms the better precision of our determinations (estimated uncertainty $\sim$ 30K).

Finally, using the higher temperatures of FAG would produce even steeper slopes in the excitation diagrams, as well as more star-to-star scatter, therefore reinforcing the problem which is the subject of the present paper.

One can thus conclude that the FAG temperatures are (1) not precise enough and (2) possibly subject to systematic errors. The latter might be due, in part, to the difficulty of obtaining reliable measurements of Balmer line wings from rather high resolution spectra, observed in pieces covering a limited spectral range. On the other hand, they may also be related to the inadequacy of the classical model atmospheres in representing the temperature stratification of metal-poor dwarfs. This inadequacy has been noted by FAG, but had already been discussed, e.g., by Magain (1984a, 1985). The correction adopted by FAG, i.e. a decrease of the mixing length parameter of convection, may be too naive to yield reliable models.

In conclusion, if we cannot definitely rule out the explanation of the mean abundance discrepancy in terms of a systematic error in the effective temperature calibration, the available evidence rather suggests that another explanation has to be searched for.

On the other hand, the scatter in the derived δ[Fe/H] amounts to 0.10 dex. One might ask whether it could be explained by random errors in the adopted $T_{\rm eff}$, caused by errors in the photometric indices. The scatter of 0.10 dex in δ[Fe/H] would corresponds to a scatter 130 K in $T_{\rm eff}$, which may be compared to the expected uncertainty. As mentioned in Section 3.1., the scatter in $T_{\rm eff}(b-y) - T_{\rm eff}(V-K)$ amounts to 39 K, which corresponds to a one sigma uncertainty of 28 K on the adopted mean temperature. The observed scatter is thus nearly five times larger than expected on these grounds, ruling out the hypothesis of random effective temperature errors as the cause of the abundance discrepancies.

This conclusion is further supported by the fact that low excitation lines of Ti I and Cr I behave like the high excitation Fe I lines, *not* like the Fe I lines having the same sensitivity, as would be expected in case of effective temperature errors (see Sect. 5).

6.3. Errors affecting a single line in all stars

Here, we consider the errors in the adopted line data, mainly oscillator strengths (damping constants play no significant role as the lines considered are quite weak). It should be mentioned that such errors would affect all δ[Fe/H] in the same way, so that the mean value could be changed, but not the star-to-star scatter. In particular, Figs. 5 and 6 would be basically unchanged. Our main conclusions would thus remain valid.

The oscillator strengths are obtained from two sources: laboratory measurements for the low EP lines and the solar spectrum for high EP ones. The Blackwell et al. measurements are of very high precision (better than one percent) so that they introduce no significant uncertainty on δ[Fe/H].

As already mentioned, the gf values of the high EP lines were derived from the solar EWs, using the HM model. This particular choice of a solar model should introduce no major uncertainty: the use of a solar model from the same grid as the stellar models would lead to a change of 0.015 dex only in the derived gf values.

A more important effect could be related to the choice of the solar abundance of iron, abundance which must be known in order to determine the gf values from the solar EWs. We adopted a value of 7.68, as deduced from low EP Fe I lines with Oxford gf values.

However, this abundance is significantly higher than the value of 7.51 derived from meteorites, and which seems to be confirmed by recent analyses of Fe II and high EP Fe I lines in the solar atmosphere (albeit with slightly less precise gf values: see Holweger et al. 1990, 1991; Biémont et al. 1991; Hannaford et al. 1992).

If we had adopted a value of 7.51 for the solar abundance of iron used in the derivation of the gf-values of the high excitation lines, i.e. the value indicated by the analyses mentioned above, our solar gf-values would have been increased by 0.17 dex. As a consequence, all our δ[Fe/H] would have been reduced by that same amount. The mean δ[Fe/H] for metal-poor stars would then be close to zero, but the star-to-star scatter would remain unchanged. In particular, as we already mentioned, the correlations shown in Figs. 4 and 5 would remain.

A comparison of our solar gf-values for the high excitation lines ($\chi_{exc} > 3$ eV) with recent laboratory measurements gives unclear results. We have one line in common with Bard et al. (1991), i.e. the 5217.4 Å line (χ_{exc} = 3.21 eV), and three lines in common with O'Brian et al. (1991): the same 5217.4 Å line, plus the 5242.5 Å (χ_{exc} = 3.63 eV) and the 5856.09 Å (χ_{exc} = 4.29 eV). Our gf-value for the first line is in perfect agreement with Bard et al. (within 0.01 dex), while the O'Brian et al. value is 0.1 dex lower. On the other hand, our gf-values for the other two lines are lower then those of O'Brian et al., by 0.22 and 0.34 dex. It should be mentioned, however, that the latter line, which is quite suitable for a derivation of the solar abundance of iron (EW = 34 mÅ), gives a very low value of 7.34 if the O'Brian et al. oscillator strength is used. This strongly suggests that the O'Brian et al. gf-value for that line is subject to caution.

On the basis of the data presently available, it is impossible to decide with any confidence if our solar gf-values for the high excitation lines are either on the right scale or some 0.17 dex too high.

The fact that the adoption of a solar abundance of 7.51, in agreement with the meteoritic value and with recent studies, would nearly cancel our mean δ[Fe/H] for metal-poor stars could be considered as an indirect argument supporting that value for the solar abundance of iron. In this case, one would argue that the low excitation Fe lines are strongly subject to departures from the excitation equilibrium in the *solar* atmosphere, while the departures would generally be weaker in metal-poor stars.

7. Consequences for the abundance analyses

The aim of the present section is to investigate the consequences of the departures from excitation equilibrium for the classical abundance analyses of metal-poor stars. These consequences may be particularly important in some cases since the lines for which the oscillator strengths are best known are just those which seem to be most affected by these effects.

Let us consider the following classical abundance analysis, whose aim is to determine the relative abundance [M/Fe] of some element M which is, like Fe, nearly fully ionized in the star's atmosphere (this is the case for most elements which are considered in such analyses, the most notable exception being the CNO elements). The model temperature is deduced from some colour index and may thus be supposed known a priori, independently of the line analysis. The surface gravity is determined by forcing the Fe II lines to indicate the same abundance as the Fe I lines. As the neutral lines are, in first approximation, independent of the surface gravity while the ionic lines vary strongly with the latter, and as the gravity is chosen in order to force consistency of the abundances, the iron abundance is fixed by the neutral lines alone and does not depend on the surface gravity.

Let us now consider two versions of this classical analysis. The first version (let us call it the H version) uses high excitation Fe I lines only, while the second version (the L version) considers exclusively low excitation lines. Following the results of Sect. 5.2, the H version is assumed to give the correct iron abundance. The errors introduced by the use of low excitation lines will be examined in two cases: (1) when the M abundance is deduced from neutral lines and (2) when it is determined on the basis of ionic lines.

7.1. Neutral lines

As the Fe and the M abundances are deduced from neutral lines, they are both insensitive to the choice of surface gravity. The Fe abundance obtained in the L version being affected by an error $-\delta$ (in general, $\delta > 0$), the relative abundance [M/Fe] will be in error by an amount δ. The use of low excitation Fe I lines will thus lead generally to an overestimate of the relative abundances deduced from neutral lines (which is the case for most of the lighter elements: e.g. Na, Mg, Al, Ca, Ti, Cr, Mn, Ni,...), provided that no departure from excitation equilibrium affects the M lines. As an example, our sample of 13 stars would indicate [Ca/Fe] = +0.45 ± 0.13 if the 0.1 eV lines were used, while a value of +0.31 ± 0.06 would be deduced from the 4.5 eV lines. (The error mentioned is the standard deviation of the individual values). This effect may thus explain, at least partly, the discrepancies in the relative abundances of the α elements, as given, e.g., by Magain (1989) and Gratton & Sneden (1988).

However, note that another contribution to the discrepancy may come from the variation of [Ca/Fe] with [Fe/H], as already suggested by Lambert (1989). This is confirmed by our results which show, when the 4.5 eV Fe I lines are used, a systematic increase of [Ca/Fe] as [Fe/H] decreases. A linear least squares fit to our data gives [Ca/Fe] = +0.15 – 0.12 [Fe/H], the scatter around this straight line amounting to 0.04 dex only.

7.2. Ionic lines

As the Fe abundance is always the one indicated by the neutral lines and as the M abundance is now obtained from ionic lines, [M/Fe] is sensitive to the adopted surface gravity. However, the latter is determined in order to bring the Fe II lines in agreement with the Fe I lines considered. Thus, in the L version, a wrong value of the surface gravity will be obtained. Changing from the right value (version H) to the wrong value (version L) of the gravity, the abundance indicated by the Fe II lines will thus change by a value $-\delta$ (the difference between the Fe abundances deduced from the low and high excitation Fe I lines). But, to a first approximation, all ionic lines have the same sensitivity to surface gravity. Thus, the M abundance, being determined from M II lines, will be in error by the same amount $-\delta$ as the Fe abundance. As a consequence, the relative abundance [M/Fe] will not be affected.

Whichever Fe I lines are chosen is thus irrelevant for the relative abundances deduced from ionic lines, as long as the surface gravity is chosen to satisfy the iron ionization equilibrium. The use of low excitation Fe I lines should not affect the relative abundances of, e.g., Sc and most heavy elements (Sr, Y, Zr, Ba, Eu,...).

Incidentally, this discussion also makes it clear that, in fact, the relative abundance, when deduced from M II lines, depends on the iron abundance indicated by the Fe II lines and is, to first order, independent of the Fe I lines which just fix the values of [Fe/H] and log g. [M/Fe] is thus in this case sensitive to the choice of the Fe II oscillator strengths which are, unfortunately, generally not well known.

8. Concluding remarks

Our empirical study of metal-poor dwarfs has shown that the Fe I lines are not formed according to the classical assumptions. It has also presented strong arguments pointing to the low excitation lines as being the ones which are affected by the departures from these assumptions. Our results indicate further that non-LTE effects might play a significant (if not dominant) role. This last conclusion is supported not only by the observed trends with effective temperature and surface gravity but also by the comparison of Fe with Ca, Ti and Cr.

However, non-LTE calculations seem to indicate that the observed effect might be slightly too large to be explained by departures from LTE alone (see, e.g., Edvardsson et al. 1993, and references therein). It should be kept in mind that temperature inhomogeneities are expected to be rather important and may play a role. Some kind of coupling between non-LTE and convection might be required to fully explain the observations. In any case, we feel that the ball is in the theoreticians' camp. Let us hope that our results will provide encouragements to those who have chosen to tackle these computationally huge problems.

Acknowledgements. This work was partially carried out during a visit of PM at the Beijing Astronomical Observatory. The Chinese NSFC and the Belgian FNRS are thanked for financial support. We also wish to thank P.E. Nissen for useful remarks

References

Bard, A., Kock, A., Kock, M. 1991, A&A 248, 315

Biémont, E., Baudoux, M., Kurucz, R.L. et al., 1991, A&A 249, 539

Blackwell, D.E., Ibbetson, P.A., Petford, A.D., Shallis, M.J. 1979a, MNRAS 186, 633

Blackwell, D.E., Petford, A.D., Shallis, M.J. 1979b, MNRAS 186, 657

Blackwell, D.E., Petford, A.D., Shallis, M.J., Simmons, G.J. 1980, MNRAS 191, 445

Blackwell, D.E., Petford, A.D., Shallis, M.J., Simmons, G.J. 1982, MNRAS 199, 43

Carney, B.W. 1983, AJ 88, 623

Delbouille, L., Neven, L., Roland, G. 1973, Photometric Atlas of the Solar Spectrum from 3000 Å to 10000 Å, Institut d'Astrophysique de l'Université de Liège, Belgium

Edvardsson, B., Andersen, J., Gustafsson, B. et al., 1993, A&A 275, 101

Fuhrmann, K., Axer, M., Gehren, T. 1993, A&A 271, 451

Gigas, D. 1988, in IAU Symposium 132, *The Impact of High S/N Spectroscopy on Stellar Physics*, eds. G. Cayrel de Strobel and M. Spite, p. 395

Gratton, R.G., Sneden, C. 1988, A&A 204, 193

Gray, D.F. 1976, *The Observation and Analysis of Stellar Photospheres*, Wiley, New York

Gustafsson, B. 1988, in IAU Symposium 132, *The Impact of High S/N Spectroscopy on Stellar Physics*, eds. G. Cayrel de Strobel and M. Spite, p. 333

Gustafsson, B., Bell, R. A., Eriksson, K., Nordlund, Å. 1975, A&A 42, 407

Hannaford, P., Lowe, R.M., Grevesse, N., Noels, A. 1992, A&A 259, 301

Holweger, H., Müller, E.A. 1974, Solar Phys. 39, 19

Holweger, H., Heise, C., Kock, M. 1990, A&A 232, 510

Holweger, H., Bard, A., Kock, A., Kock, M. 1991, A&A 249, 545

King, J.R. 1993, AJ 106, 1206

Lambert, D. L. 1989, in *Cosmic Abundances of Matter*, AIP Conf. Proc., No. 183, p. 168

Magain, P. 1983, A&A 122, 225

Magain, P. 1984a, A&A 132, 208

Magain, P. 1984b, A&A 134, 189

Magain, P. 1985, A&A 146, 95

Magain, P. 1987, A&A 181, 323

Magain, P. 1988, in IAU Symposium 132, *The Impact of High S/N Spectroscopy on Stellar Physics*, eds. G. Cayrel de Strobel and M. Spite, p. 485

Magain, P. 1989, A&A 209, 211

Nordlund, Å. 1984, in *Small Scale Dynamic Processes in Quiet Stellar Atmospheres*, ed. S.L. Keil, Sacramento Peak, Sunspot, New Mexico, p. 30

O'Brian, T.R., Wickliffe, M.E., Lawler, J.E. et al., 1991, JOSA B 8, 1185

Peterson, R. C. 1988, in IAU Symposium 132, *The Impact of High S/N Spectroscopy on Stellar Physics*, eds. G. Cayrel de Strobel and M. Spite, p. 493

Ruland, F., Holweger, H., Griffin, R. et al., 1980, A&A 92, 70

Schuster, W.J., Nissen, P.E. 1988, A&ASS 73, 225

Simmons, G.J., Blackwell, D.E. 1982, A&A 112, 209

Smith, G. 1981, A&A 103, 351

Smith, G., Raggett, D. St. J.: 1981, J. Phys. B 14, 4015

Steffen, M. 1985, A&ASS 59, 403

VandenBerg, D.A., Bell, R.A. 1985, ApJSS 58, 561

This article was processed by the author using Springer-Verlag LaTeX A&A style file version 3.